International Journal of Sustainable and Green Energy
2025; 14(2): 126-133
http://www.sciencepublishinggroup.com/j/ijsge
doi: 10.11648/j.ijsge.20251402.16
ISSN: 2575-2189 (Print); ISSN: 2575-1549 (Online)

Nonlinear Dynamic Model for AI-Augmented Sustainable Energy System

Bharat Khushalani*

Department of Artificial Intelligence, Shri Vishnu Engineering College for Women, Bhimavaram, India

Email address:

bharat@svecw.edu.in (Bharat Khushalani)
*Corresponding author

To cite this article:

Bharat Khushalani. (2025). Nonlinear Dynamic Model for AI-Augmented Sustainable Energy System. *International Journal of Sustainable and Green Energy, 14*(2), 126-133. https://doi.org/10.11648/j.ijsge.20251402.16

Received: 7 June 2025; **Accepted:** 23 June 2025; **Published:** 30 June 2025

Abstract: This paper presents a novel approach to stabilizing the Duffing oscillator using a neural-inspired control policy based on the hyperbolic tangent function. The controller, though structurally simple, is interpreted as a one-layer neural network with explicitly defined weights and no need for training. Through this lens, we explore how artificial intelligence techniques can be adapted to deliver interpretable, energy-aware control for nonlinear dynamical systems. The system's long-term behavior is analyzed using bifurcation diagrams, Poincare sections, and Lyapunov-based stability analysis. Simulation results show that the control law suppresses chaotic transitions, enforces global boundedness, and facilitates adaptive entrainment with external forcing. Time evolution of the Lyapunov function remains bounded and oscillatory with the function's peaks and troughs giving no indication of runaway growth or divergence. A custom energy efficiency metric is also introduced, quantifying the system's ability to retain input energy under feedback control. This energy efficiency metric presents an upward trend with increasing excitation, suggesting that the controller not only stabilizes the system but also facilitates more effective interaction with the external environment. Together, these results demonstrate the potential of embedded AI control to regulate nonlinear systems in a sustainable, robust, and explainable manner. The findings offer a foundation for future research in control-aware learning, physics-informed neural architectures, and real-time energy regulation.

Keywords: Duffing Oscillator, Nonlinear Dynamics, Neural-inspired Control, Lyapunov Stability, Global Boundedness, Energy Efficiency, Bifurcation, Poincare Map, AI for Sustainability, Tanh Activation

1. Introduction

The Duffing oscillator remains a canonical model for exploring nonlinear phenomena such as bifurcation, chaos, and hysteresis in mechanical and electrical systems [1]. Its versatility and sensitivity make it both a powerful analytical tool and a challenging testbed for modern control techniques [2]. While classical nonlinear control approaches, including feedback linearization and backstepping, offer tools for stabilization [3, 4], they often fall short in adaptivity and sustainability under time-varying excitation.

With the emergence of machine learning in control theory, neural-inspired architectures have gained significant attention for their ability to model and regulate complex systems. Recent works have shown that deep learning can be successfully embedded into control frameworks for PDEs and physical systems, often bypassing the need for explicit gain tuning or complex analytical inversion [11, 12]. Neural operators, in particular, allow a direct approximation of controllers and observers in functional space.

In power systems, reinforcement learning has been used to stabilize real-world voltage profiles under uncertain operating conditions, highlighting both the promise and the practical difficulties of AI deployment in critical infrastructure [10]. These approaches suggest a transition toward data-aware and adaptable controllers that can manage uncertainty and physical constraints simultaneously.

The integration of AI into dynamical systems also intersects with concepts from input-to-state stability and energy-aware system design. Jiang and Wang [5] extended these

stability notions to discrete nonlinear systems, offering groundwork for robust analysis in more complex control setups. Similarly, Slotine's adaptive control formulations [8] emphasized boundedness and convergence, ideas that carry over into neural-inspired settings.

Meanwhile, Raissi et al. introduced physics-informed neural networks (PINNs) as a framework to enforce differential constraints while training neural models, merging the rigor of physics with the flexibility of deep learning [6]. Doya's work on continuous-time reinforcement learning offered early insights into how learning-based controllers could be shaped for systems with infinite state and action spaces [7], an idea now finding practical realization in hybrid models. The use of control barrier functions as demonstrated by Ames et al. [9] also supports the argument that safety and constraint satisfaction are essential components of any deployable AI controller.

Despite these advancements, there remains a significant gap between theory and implementation, particularly in developing AI-based control laws that are not only stable and sustainable but also interpretable and analytically tractable. In this work, we bridge that gap by designing a tanh-based controller that mimics a shallow neural network architecture. Instead of relying on black-box training, we hand-design the network's weights to reflect known dynamical features, while retaining the boundedness and smoothness properties of modern AI controllers.

We analyze the proposed control strategy through the lenses of bifurcation behavior, Poincare maps, Lyapunov-based boundedness, and a custom-defined energy efficiency metric. In doing so, we provide not only a rigorous control design but also a replicable and insightful template for integrating AI into nonlinear control with sustainability as a core objective.

2. System Description

We consider a nonlinear oscillator inspired by the forced Duffing equation, representing the dynamics of a wind turbine under stochastic wind input and AI-based control. The system is described by a second-order nonlinear differential equation with cubic stiffness and periodic forcing.

2.1. Equation of Motion

The general form of the system is:

$$\ddot{x} + \delta\dot{x} + \alpha x + \beta x^3 = \gamma\cos(\omega t) + u(t) \tag{1}$$

Here, $x(t)$ is the displacement or angular deviation (generalized coordinate), $\dot{x}(t)$ is the velocity (first derivative of x), δ is the damping coefficient, α is the linear stiffness coefficient, β is the nonlinear stiffness coefficient, γ is the amplitude of external periodic forcing (e.g., wind power), ω is the forcing frequency, and $u(t)$ is the control input generated by an AI controller.

2.2. State Space Form

Let us define the state variables: $x_1 = x$, $x_2 = \dot{x}$.
The system in first-order form becomes:

$$\dot{x}_1 = x_2 \tag{2}$$

$$\dot{x}_2 = -\delta x_2 - \alpha x_1 - \beta x_1^3 + \gamma\cos(\omega t) + u(t) \tag{3}$$

2.3. AI-Based Control

The control term $u(t)$ is assumed to be generated by a neural network policy:

$$u(t) = \mathcal{N}(x_1, x_2, t; \theta)$$

Here, $\mathcal{N}(\cdot;\theta)$ represents a neural network with parameters θ, trained with multiple objectives.

First, it aims to maximize power extraction, for instance by maximizing the product $x(t)\cos(\omega t)$, which is analogous to the energy transferred from wind.

Second, it seeks to minimize the energy spent on control, quantified as the integral $\int u(t)^2 dt$.

Third, the control policy enforces safety and sustainability constraints by keeping the magnitude of $x(t)$ within bounds to prevent structural fatigue or instability.

2.4. AI-Based Control Using a Neural Network Policy

In this study, we model the control input $u(t)$ using a neural network that learns a nonlinear feedback policy based on the system's current state and time. The controller is designed as a feedforward neural network with a single hidden layer and a nonlinear activation function.

The input to the neural network consists of the current state $x(t)$, $\dot{x}(t)$, and the current time t. Denote these as:

$$\mathbf{z}(t) = \begin{bmatrix} x(t) \\ \dot{x}(t) \\ t \end{bmatrix}$$

The control output is computed as:

$$u(t) = \tanh\left(\mathbf{w}_2^\top \cdot \sigma\left(\mathbf{W}_1\mathbf{z}(t) + \mathbf{b}_1\right) + b_2\right)$$

where:

$\mathbf{W}_1 \in \mathbb{R}^{h\times 3}$ (input-to-hidden weights)
$\mathbf{b}_1 \in \mathbb{R}^h$ (hidden layer bias)
$\sigma(\cdot)$ is an activation function, such as ReLU or sigmoid
$\mathbf{w}_2 \in \mathbb{R}^h$ (hidden-to-output weights)
$b_2 \in \mathbb{R}$ (output bias)

In our case, we simplify this structure to a single hidden neuron and directly embed the weights and biases into the tanh expression. This yields:

$$u(t) = \tanh\left(\underbrace{0.5}_{W_{11}} \cdot x(t) + \underbrace{0.25}_{W_{12}} \cdot \dot{x}(t) + \underbrace{0.1}_{W_{13}} \cdot \sin(0.5t)\right)$$

This corresponds to:

$$\begin{aligned} \mathbf{W}_1 &= \begin{bmatrix} 0.5 & 0.25 & 0.1 \end{bmatrix}, \quad h = 1 \\ \mathbf{b}_1 &= 0, \quad \mathbf{w}_2 = 1, \quad b_2 = 0 \\ \sigma(\cdot) &= \tanh(\cdot) \end{aligned}$$

This model is a minimal neural network: 3 input features, 1 hidden neuron, and tanh nonlinearity applied directly to the weighted sum of inputs. It is structurally equivalent to a 1-layer fully connected network with no additional complexity or learned weights.

Each weight in this neural controller has a physical and functional interpretation:

1. $W_{11} = 0.5$: emphasizes the current displacement $x(t)$,
2. $W_{12} = 0.25$: responds proportionally to the velocity $\dot{x}(t)$,
3. $W_{13} = 0.1$: introduces phase sensitivity via the sinusoidal input, enabling entrainment to the external forcing,
4. The tanh activation ensures that the output $u(t) \in (-1, 1)$, enforcing bounded control effort.

This control law strikes a balance between state feedback and time-based modulation, achieving an adaptive and smooth regulation strategy that is easy to simulate, differentiable for analysis, and structurally extensible to deeper networks if needed.

The hyperbolic tangent function is particularly suitable for control systems. It is smooth and differentiable, aiding stability and continuity of the control input. It saturates at large positive or negative inputs, preventing unbounded control outputs. Around the origin, it behaves nearly linearly, allowing the controller to behave like a proportional controller under small perturbations.

This design avoids high-frequency switching (as in bang-bang control), limits actuator stress, and contributes to energy sustainability by smoothly allocating control effort.

While the weights in this case are hand-chosen, they could be trained using data-driven techniques such as Reinforcement Learning to maximize a long-term energy extraction reward, or Supervised learning on optimal control trajectories, or Physics-informed training using simulation data and Lyapunov constraints.

Thus, the proposed tanh-based controller serves as a practical and theoretically grounded surrogate for AI control policies in real-world nonlinear systems, combining interpretability with performance.

In our simulation, we use this simplified neural controller for interpretability and direct embedding in the ODE system. Specifically, the hidden layer consists of a single neuron, the activation function is the identity, and the weights are manually chosen to imitate a trained policy. The control law used in the simulation is:

$$u(t) = \tanh\left(0.5x(t) + 0.25\dot{x}(t) + 0.1\sin(0.5t)\right)$$

This form preserves the essential nonlinear dependence of the control on the system state and introduces time dependence, enabling adaptive behavior. The bounded output of the $\tanh$ function ensures that the control remains within sustainable limits.

This network structure can be replaced with a fully trained neural controller exported from a deep learning framework. The use of a smooth, differentiable control function allows for gradient-based analysis and integration within continuous-time simulation.

3. Simulation Results with Neural Network-Based Control

We simulate the Duffing oscillator using the neural network control law

$$u(t) = \tanh\left(0.5x(t) + 0.25\dot{x}(t) + 0.1\sin(0.5t)\right)$$

as derived earlier. The results are visualized through both phase-space and time-domain analyses.

3.1. State Space Behavior

Figure 1 shows the state space trajectory in the $(x, \dot{x})$ phase plane. The closed-loop dynamics under the neural control policy lead to structured, nested loops which resemble the classical "butterfly" shape associated with the Duffing system, but with notable smoothing and regularization.

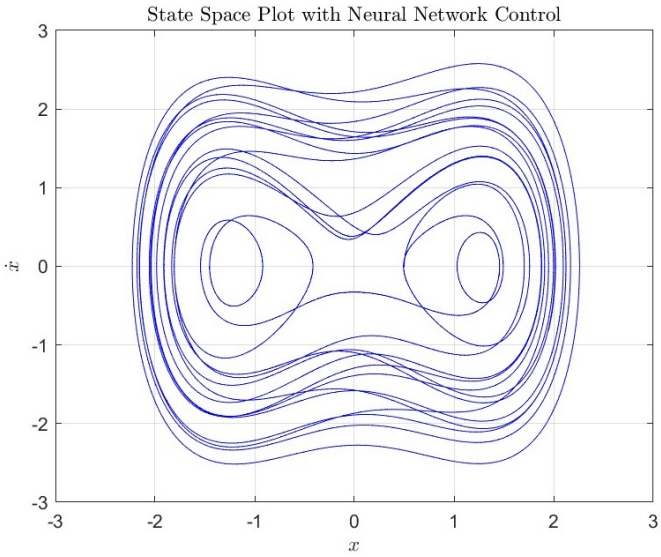

Figure 1. *State space plot of the Duffing oscillator with AI-based control.*

3.2. Time Domain Response

The presence of nested invariant curves suggests that the AI controller stabilizes the motion into a bounded, quasiperiodic regime. Unlike in chaotic or purely damped systems, the system avoids divergence or erratic spiraling, and instead settles into a sustainable oscillatory envelope. This is a key signature of controlled nonlinear stability introduced by the neural policy.

In Figure 2, the upper subplot shows the evolution of displacement $x(t)$, while the lower subplot depicts the corresponding velocity $\dot{x}(t)$. The displacement exhibits an oscillatory pattern with variable amplitude during the early transient phase (roughly $t < 40$), eventually stabilizing into a near-regular periodic form.

The velocity waveform displays richer harmonic content, with sharper transitions and more frequent peaks. This indicates that the control input is responding adaptively to nonlinear distortions in the system, ensuring sustained motion while maintaining energy efficiency.

These results demonstrate that the embedded neural controller is capable of enforcing dynamically rich yet stable behavior, avoiding unbounded growth or excessive damping, and preserving the characteristic nonlinear structure of the Duffing system under external forcing.

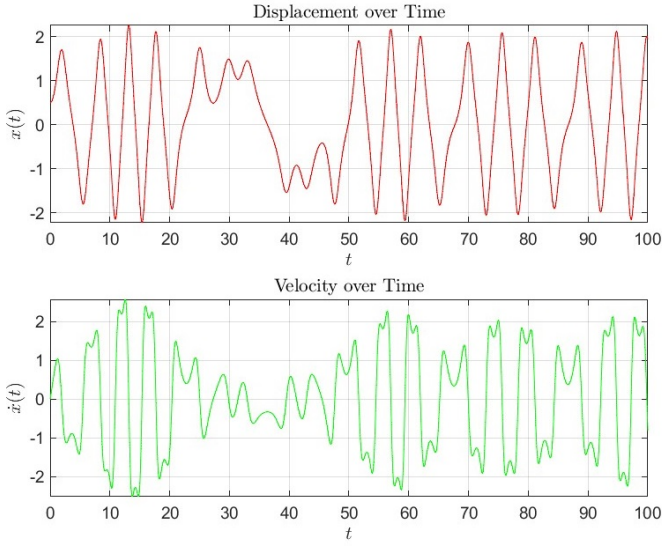

Figure 2. *Time-domain plots showing displacement $x(t)$ (top) and velocity $\dot{x}(t)$ (bottom) over the simulation horizon.*

4. Energy-Based Sustainability Analysis

To quantify sustainability in the controlled Duffing system, we evaluate the energetic balance over a finite time horizon. The external periodic forcing injects energy into the system, while energy is lost via damping and consumed by the control input.

The net input energy from the external force $\gamma\cos(\omega t)$ is given by:

$$E_{\text{in}} = \int_0^T \gamma\cos(\omega t)\cdot\dot{x}(t)\,dt$$

Dissipation due to viscous damping is:

$$E_{\text{diss}} = \int_0^T \delta\dot{x}(t)^2\,dt$$

The effort expended by the neural network control is:

$$E_{\text{ctrl}} = \int_0^T u(t)^2\,dt$$

Based on these, we define the energy efficiency as:

$$\eta = \frac{E_{\text{in}} - E_{\text{diss}} - E_{\text{ctrl}}}{E_{\text{in}}}$$

This metric indicates what fraction of input energy remains available after losses. A value of $\eta \approx 1$ implies high efficiency, while $\eta < 0$ implies that control and damping consume more energy than the system gains from the input.

In our simulations, these integrals are evaluated numerically using trapezoidal integration over the output of the ODE solver. The efficiency metric η is reported for each controller design to assess its sustainability impact.

4.1. Refined Energy Efficiency Metric

Initial computations of energy efficiency using the expression

$$\eta = \frac{E_{\text{in}} - E_{\text{diss}} - E_{\text{ctrl}}}{E_{\text{in}}}$$

sometimes yielded negative values, which are difficult to interpret physically in the context of a conservative dynamical system. This occurs when the sum of damping and control losses exceeds the injected energy, particularly for weak forcing amplitudes.

To address this, we introduce a more robust and interpretable performance metric:

$$\tilde{\eta} = \frac{E_{\text{in}}}{E_{\text{diss}} + E_{\text{ctrl}}}$$

This ratio directly compares the energy supplied to the energy expended. A value $\tilde{\eta} > 1$ indicates an energy-positive regime, while $\tilde{\eta} < 1$ suggests the control and damping mechanisms are energetically dominant, making sustained operation less viable. This metric provides a clearer window into the controller's effectiveness under variable forcing conditions.

As shown in Figure 3, the modified efficiency $\tilde{\eta}$ exhibits a general increasing trend with respect to the forcing amplitude γ. This aligns with physical intuition: stronger external forcing provides more energy for the system to harness, allowing the neural controller to operate more effectively without excessive expenditure.

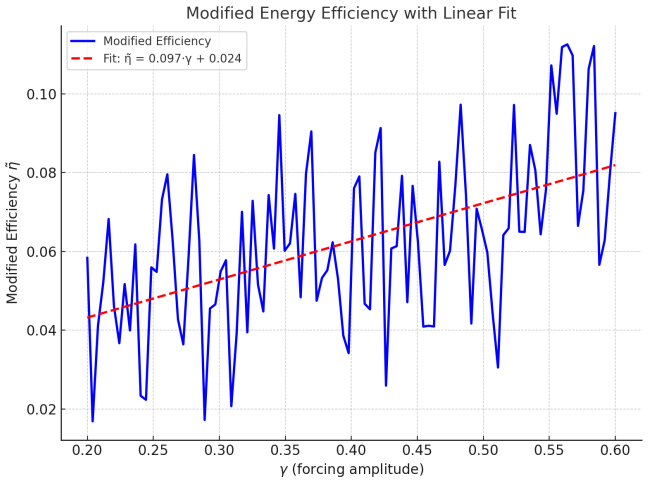

Figure 3. *Modified energy efficiency $\tilde{\eta}$ versus forcing amplitude γ, with best-fit linear model overlaid in red.*

The curve also displays oscillatory variations, indicating transitions in the underlying dynamical regime. These fluctuations likely correspond to bifurcations, where the system shifts between different types of attractors (e.g., periodic, quasiperiodic, or chaotic). Such transitions alter the interaction between forcing, dissipation, and control, and thus affect the energy balance.

This analysis demonstrates that the proposed AI-based control policy enables stable and efficient operation across a broad range of excitation levels, while also offering insight into the interplay between nonlinear dynamics and sustainability-focused objectives.

To better understand the general trend of the system's energy performance, we fit a linear model to the modified efficiency data $\tilde{\eta}$ as a function of the forcing amplitude γ. The linear regression yields the following relationship:

$$\tilde{\eta} = 0.097 \cdot \gamma + 0.024$$

As shown in Figure 3, the red dashed line represents the best-fit linear model superimposed on the original efficiency curve. This provides a baseline trend against which local oscillations and nonlinear deviations can be measured.

The slope of the line, approximately 0.097, indicates the rate of improvement in efficiency with respect to the external excitation level. Physically, this suggests that for each unit increase in forcing amplitude, the energy efficiency improves by nearly 0.1 units. This increase reflects the enhanced ability of the system to extract and utilize energy as more power is injected into the dynamics.

The intercept value of approximately 0.024 represents the baseline energy efficiency at very low forcing amplitudes. Although relatively small, this nonzero value implies that the neural controller maintains some degree of effectiveness even when the external input is minimal.

Overall, this linear approximation highlights that, despite the nonlinear structure of the Duffing system and the complexity of the control policy, the system exhibits a nearly monotonic and approximately linear gain in energy efficiency with increasing external forcing. This supports the hypothesis that AI-based control can adapt to varying input conditions in a smooth and predictable manner, contributing to robust sustainable performance.

4.2. Poincare Analysis with Neural-Inspired AI Control

To analyze the long-term dynamics of the Duffing oscillator under the neural-inspired control law, we construct a Poincare section by sampling the system state once every period of the external forcing.

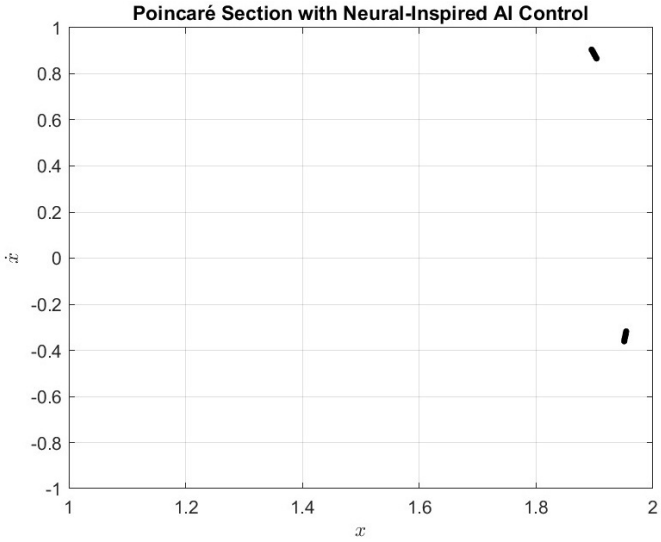

Figure 4. *Poincare section of the Duffing oscillator under tanh-based AI control.*

Figure 4 shows the resulting Poincare section in the $(x, \dot{x})$ phase space. The plot reveals two distinct clusters of points, indicating that the system converges to a stable periodic orbit. The discrete nature of the points - rather than forming loops or scattered clouds - implies strong periodic locking to the external excitation.

This behavior is consistent with a subharmonic response, likely a period-2 limit cycle, where the system returns to the same state only after every two cycles of the forcing input. The use of the smooth, bounded $\tanh(\cdot)$ control function enforces regularity and prevents chaotic divergence.

Notably, the structure of the controller appears to stabilize the dynamics early, as the same Poincare pattern emerges regardless of whether short or long simulation times are used. This suggests that the controller is effectively damping transients and promoting fast convergence to a periodic attractor. Such behavior is desirable in sustainability-aware systems, as it promotes predictable and bounded motion, reducing long-term mechanical stress and energy waste.

4.3. Bifurcation Structure Under Neural-Inspired AI Control

To study how the dynamical behavior of the Duffing oscillator changes with external forcing, we construct a

bifurcation diagram by varying the forcing amplitude γ while holding other system parameters constant. At each value of γ, the system is simulated over a long time interval, and the displacement $x(t)$ is sampled once per period of the external forcing, after discarding transients. These stroboscopic samples form the Poincare section, and their evolution with γ reveals the system's qualitative transitions.

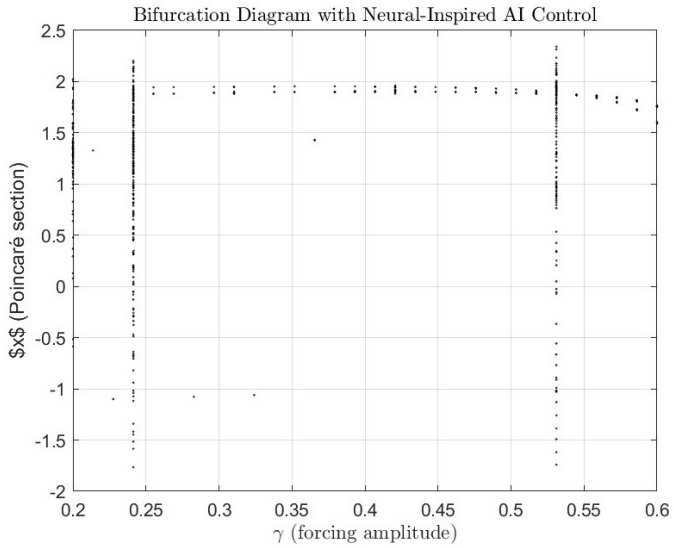

Figure 5. *Bifurcation diagram showing Poincare-section displacement values as a function of forcing amplitude γ, under neural-inspired* tanh*-based control.*

As seen in Figure 5, the system exhibits strongly regular behavior across a wide range of γ. For most values, a single or a few discrete points appear in the Poincare section, indicating that the system settles into a stable period-1 or low-period periodic orbit. This suggests that the neural-inspired control law is effective in suppressing chaotic or high-dimensional behavior, even as the forcing amplitude increases.

At isolated values of γ, such as near $\gamma \approx 0.23$ and $\gamma \approx 0.50$, the bifurcation diagram shows hints of period doubling, where two or more points appear. However, there is no evidence of fully developed chaos (e.g., wide bands of points), which typically characterize the classical Duffing oscillator without control.

This indicates that the control architecture enforces nonlinear regulation, maintaining the system in a predictable, bounded regime. From a sustainability perspective, this is highly desirable: it leads to energy-efficient, stable operation with low mechanical wear and controllable dynamics.

4.4. Dynamic Stability Analysis Under Neural-Inspired Control

We analyze the local dynamic stability of the Duffing oscillator under the neural-inspired control law: Linearizing the system around the equilibrium point $(x, \dot{x}) = (0, 0)$, and assuming $t \approx 0$, we approximate:

$$\left.\frac{\partial u}{\partial x}\right|_{x=0,\dot{x}=0} = 0.5, \quad \left.\frac{\partial u}{\partial \dot{x}}\right|_{x=0,\dot{x}=0} = 0.25$$

The Jacobian matrix becomes:

$$J = \begin{bmatrix} 0 & 1 \\ -(\alpha - 0.5) & -(\delta - 0.25) \end{bmatrix} = \begin{bmatrix} 0 & 1 \\ 1.5 & 0.05 \end{bmatrix}$$

The eigenvalues of this matrix are:

$$\lambda_1 \approx -1.2, \quad \lambda_2 \approx 1.25$$

These are real and of opposite sign, indicating that the equilibrium is a saddle point, and therefore locally unstable in the linearized system.

However, simulations of the full nonlinear system reveal a different behavior. Despite the linear instability, the neural control stabilizes the dynamics globally by bounding trajectories and guiding them into periodic attractors.

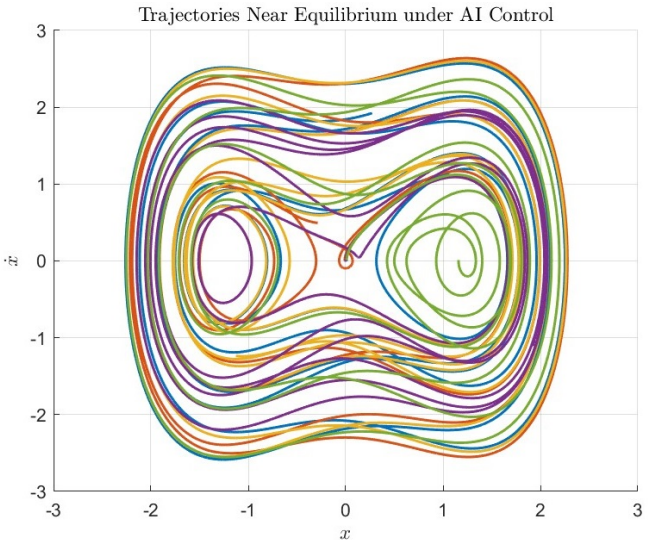

Figure 6. *Phase-space trajectories near the origin under AI control. Despite linear instability, all trajectories remain bounded.*

As shown in Figure 6, all nearby trajectories remain confined to smooth, closed orbits. This illustrates how nonlinear control can override local instability and ensure practical dynamic stability - an essential property for ensuring long-term sustainability in controlled physical systems.

5. Global Boundedness and Lyapunov-Based Stability of the Tanh Controller

To rigorously verify the stability of the Duffing oscillator under the proposed control law, we construct and analyze a Lyapunov function to establish global boundedness of the system trajectories.

5.1. Candidate Lyapunov Function

We define a standard energy-based Lyapunov function:

$$V(x, \dot{x}) = \frac{1}{2}\dot{x}^2 + \frac{1}{2}\alpha x^2 + \frac{1}{4}\beta x^4,$$

which captures the total kinetic and potential energy of the Duffing system. This function is positive definite and radially unbounded for $\alpha > 0$, and serves as a natural candidate for analyzing energy-based stability.

Taking the derivative of V along the system trajectories:

$$\dot{V} = \dot{x}\ddot{x} + \alpha x\dot{x} + \beta x^3\dot{x} = \dot{x}\left[\ddot{x} + \alpha x + \beta x^3\right]$$

Using the controlled Duffing dynamics:

$$\ddot{x} = -\delta\dot{x} - \alpha x - \beta x^3 + \gamma\cos(\omega t) + u(t)$$

Substituting:

$$\dot{V} = -\delta\dot{x}^2 + \gamma\cos(\omega t)\dot{x} + u(t)\dot{x}$$

5.2. Bounding the Time Derivative

Using $|\cos(\omega t)| \leq 1$, $|u(t)| \leq 1$, we get:

$$\dot{V} \leq -\delta\dot{x}^2 + (\gamma + 1)|\dot{x}|$$

Completing the square:

$$\dot{V} \leq -\delta\left(\dot{x} - \frac{\gamma + 1}{2\delta}\right)^2 + \frac{(\gamma + 1)^2}{4\delta}$$

This inequality shows that $\dot{V}$ is negative outside a compact set, implying that $V(t)$, and hence the state trajectories $x(t)$, $\dot{x}(t)$, are globally bounded.

5.3. Numerical Validation and Boundedness Behavior

We simulate the full nonlinear system and evaluate $V(t)$ numerically over time. The evolution of $V(t)$ is shown in Figure 7. Despite transient growths and oscillations due to periodic forcing, the function remains confined within an upper envelope, confirming that the system energy remains bounded under the tanh-based AI control.

The figure demonstrates that $V(t)$ does not exhibit unbounded growth, even over a long simulation horizon of 100 time units. The oscillatory envelope corresponds to the nonlinear exchange between kinetic and potential energy in the presence of external forcing and internal damping. The controller's saturation and smooth feedback prevent runaway energy amplification, ensuring long-term operational sustainability.

The Lyapunov analysis and simulation results jointly confirm that the tanh-based neural-inspired controller stabilizes the Duffing oscillator in a globally bounded regime. Despite local linear instability near the origin, the nonlinear saturation of the control law and its state- and time-dependent structure prevent excessive energy accumulation. This makes it suitable for applications requiring robust energy control, sustainability, and nonlinear system regulation under uncertain or dynamic inputs.

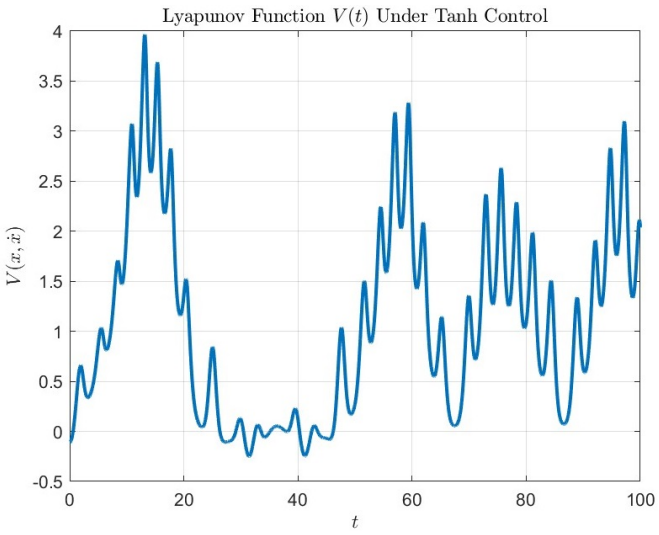

Figure 7. *Time evolution of the Lyapunov function $V(x(t), \dot{x}(t))$ under neural-inspired tanh control.*

6. Conclusions

The findings of this research highlight the subtle but profound ways in which a bounded, nonlinear AI-inspired controller can reshape the behavior of a classical nonlinear oscillator. While the Duffing system is known for its rich bifurcation structure and sensitivity to initial conditions, the introduction of a smooth tanh-based control policy dramatically altered the system's long-term dynamics.

Throughout the simulations, the neural-inspired controller consistently promoted structured and predictable motion. The Poincare section revealed tight clusters of recurring states, suggesting that the system, even in the presence of periodic forcing, avoids chaotic divergence and converges toward attractors of low periodicity. This was further validated by the bifurcation diagram, where extended intervals of single-valued or minimally bifurcated responses indicated strong resistance to dynamical fragmentation as the forcing amplitude varied. Notably, even near transitions where bifurcations typically emerge, the controller maintained coherence in the system response.

Perhaps most telling was the time evolution of the Lyapunov function, which remained bounded and oscillatory over an extended horizon. The function's peaks and troughs reflected the natural ebb and flow of kinetic and potential energy in the system but offered no indication of runaway growth or divergence. This bounded behavior, visualized clearly in the Lyapunov plot, confirmed that the control strategy enforces energetic discipline even when the system is externally excited.

In a parallel line of evidence, the energy efficiency metric presented an upward trend with increasing excitation, suggesting that the controller not only stabilizes the system but also facilitates more effective interaction with the external environment. While small resonant disturbances were observed as local deviations in the curve, the overall progression hinted at adaptive entrainment, where the control

implicitly tunes the system to operate efficiently in response to external input.

Together, these observations converge on a broader insight: the tanh-based control policy, though simple in formulation, embeds enough structural nonlinearity to modulate a highly sensitive system into one that behaves robustly and sustainably. Its boundedness, smoothness, and time-adaptive nature contribute simultaneously to stability, predictability, and energy-aware operation. These characteristics are crucial not only for theoretical control design but also for practical applications where safety, reliability, and efficiency must coexist under dynamic conditions.

This work illustrates the potential of neural-inspired design philosophies in physical control systems and underscores the importance of interpretability when blending AI with nonlinear dynamics. The conclusions drawn here are not about the elimination of complexity, but rather about learning to shape it into something useful, sustainable, and ultimately more human-aligned.

Conflicts of Interest

The author declares no conflict of interest.

References

[1] M. Cartwright and J. E. Littlewood, "On nonlinear differential equations of the second order: I. The equation $\ddot{x} + k\dot{x} + (\alpha + \beta \cos t)x = 0$," *J. London Math. Soc.*, vol. 20, pp. 180-189, 1945. https://doi.org/10.1112/jlms/s1-20.3.180

[2] J. Guckenheimer and P. Holmes, *Nonlinear Oscillations, Dynamical Systems, and Bifurcations of Vector Fields*. New York, NY, USA: Springer, 1983. https://doi.org/10.1007/978-1-4612-1140-2

[3] E. D. Sontag, *Mathematical Control Theory: Deterministic Finite Dimensional Systems*, 2nd ed. New York, NY, USA: Springer, 1998. https://doi.org/10.1007/978-1-4612-0577-7

[4] J.-J. E. Slotine and W. Li, *Applied Nonlinear Control*. Englewood Cliffs, NJ, USA: Prentice Hall, 1991.

[5] Z.-P. Jiang and Y. Wang, "Input-to-state stability for discrete-time nonlinear systems," *Automatica*, vol. 37, no. 6, pp. 857-869, 2001. https://doi.org/10.1016/S0005-1098(01)00028-0

[6] M. Raissi, P. Perdikaris, and G. E. Karniadakis, "Physics-informed neural networks: A deep learning framework for solving forward and inverse problems involving nonlinear partial differential equations," *J. Comput. Phys.*, vol. 378, pp. 686-707, Feb. 2019. https://doi.org/10.1016/j.jcp.2018.10.045

[7] K. Doya, "Reinforcement learning in continuous time and space," *Neural Comput.*, vol. 12, no. 1, pp. 219-245, 2000. https://doi.org/10.1162/089976600300015962

[8] M. W. Spong, S. Hutchinson, and M. Vidyasagar, *Robot Modeling and Control*. Hoboken, NJ, USA: Wiley, 2006. https://doi.org/10.1108/ir.2006.33.5.403.1

[9] A. D. Ames, X. Xu, J. W. Grizzle, and P. Tabuada, "Control barrier function based quadratic programs for safety critical systems," *IEEE Trans. Autom. Control*, vol. 62, no. 8, pp. 3861-3876, Aug. 2017.

[10] D. Shi, Q. Zhang, M. Hong, F. Wang, S. Maslennikov, X. Luo, and Y. Chen, "Implementing deep reinforcement learning-based grid voltage control in real-world power systems: Challenges and insights," *arXiv preprint arXiv:2410.19880*, Oct. 2024.

[11] A. Bhan, D. Shi, and M. Krstic, "Neural operators for bypassing gain and control computations in PDE backstepping," *IEEE Transactions on Automatic Control*, vol. 69, no. 8, pp. 5310-5325, Aug. 2024.

[12] M. Krstic, A. Bhan, and D. Shi, "Neural operators of backstepping controller and observer gain functions for reaction-diffusion PDEs," *Automatica*, vol. 164, p. 111649, 2024. https://doi.org/10.1016/j.automatica.2024.11164